THE JOURNAL OF IMMUNOLOGY

Airway and Lung Pathology Due to Mucosal Surface Dehydration in β-Epithelial Na^+ Channel-Overexpressing Mice: Role of TNF-α and IL-4R α Signaling, Influence of Neonatal Development, and Limited Efficacy of Glucocorticoid Treatment

Alessandra Livraghi, Barbara R. Grubb, Elizabeth J. Hudson, Kristen J. Wilkinson, John K. Sheehan, Marcus A. Mall, Wanda K. O'Neal, Richard C. Boucher and Scott H. Randell

J Immunol 2009;182;4357-4367
doi:10.4049/jimmunol.0802557
http://www.jimmunol.org/content/182/7/4357

The Journal of Immunology is published twice each month by
The American Association of Immunologists, Inc.,
9650 Rockville Pike, Bethesda, MD 20814-3994.

Print ISSN: 0022-1767 Online ISSN: 1550-6606.

Airway and Lung Pathology Due to Mucosal Surface Dehydration in β-Epithelial Na^+ Channel-Overexpressing Mice: Role of TNF-α and IL-4Rα Signaling, Influence of Neonatal Development, and Limited Efficacy of Glucocorticoid Treatment[1]

Alessandra Livraghi,[2]* Barbara R. Grubb,* Elizabeth J. Hudson,* Kristen J. Wilkinson,* John K. Sheehan,* Marcus A. Mall,† Wanda K. O'Neal,* Richard C. Boucher,* and Scott H. Randell*

Overexpression of the epithelial Na^+ channel β subunit (*Scnn1b* gene, βENaC protein) in transgenic (Tg) mouse airways dehydrates mucosal surfaces, producing mucus obstruction, inflammation, and neonatal mortality. Airway inflammation includes macrophage activation, neutrophil and eosinophil recruitment, and elevated KC, TNF-α, and chitinase levels. These changes recapitulate aspects of complex human obstructive airway diseases, but their molecular mechanisms are poorly understood. We used genetic and pharmacologic approaches to identify pathways relevant to the development of *Scnn1b*-Tg mouse lung pathology. Genetic deletion of TNF-α or its receptor, TNFR1, had no measurable effect on the phenotype. Deletion of IL-4Rα abolished transient mucous secretory cell (MuSC) abundance and eosinophilia normally observed in neonatal wild-type mice. Similarly, IL-4Rα deficiency decreased MuSC and eosinophils in neonatal *Scnn1b*-Tg mice, which correlated with improved neonatal survival. However, chronic lung pathology in adult *Scnn1b*-Tg mice was not affected by IL-4Rα status. Prednisolone treatment ablated eosinophilia and MuSC in adult *Scnn1b*-Tg mice, but did not decrease mucus plugging or neutrophilia. These studies demonstrate that: 1) normal neonatal mouse airway development entails an IL-4Rα-dependent, transient abundance of MuSC and eosinophils; 2) absence of IL-4Rα improved neonatal survival of *Scnn1b*-Tg mice, likely reflecting decreased formation of asphyxiating mucus plugs; and 3) in *Scnn1b*-Tg mice, neutrophilia, mucus obstruction, and airspace enlargement are IL-4Rα- and TNF-α-independent, and only MuSC and eosinophilia are sensitive to glucocorticoids. Thus, manipulation of multiple pathways will likely be required to treat the complex pathogenesis caused by airway surface dehydration. *The Journal of Immunology,* 2009, 182: 4357–4367.

Airway epithelial overexpression of the epithelial Na^+ channel β subunit (βENaC protein, *Scnn1b* gene), driven by the Clara cell secretory protein (CCSP)[3] promoter in transgenic (Tg) mice, results in epithelial Na^+ hyperabsorption, airway surface liquid (ASL) dehydration, impaired mucus clearance, airway inflammation, and early postnatal mortality (1). The *Scnn1b*-Tg mouse model recapitulates many features of cystic fibrosis (CF) and other human airway diseases associated with relative dehydration of airway surfaces (2), including chronic bronchitis (CB) and chronic obstructive pulmonary disease (COPD). At birth, the lungs of *Scnn1b*-Tg mice are morphologically normal, but they rapidly develop time-dependent abnormalities (3). Tracheal mucus obstruction is associated with neonatal mortality, and, in surviving mice, mucus plugging and mucous secretory cell (MuSC) metaplasia progressively extend into the intrapulmonary bronchi. The inflammatory infiltrate is characterized by enlarged/highly vacuolated macrophages, persistent neutrophilia associated with elevated KC, MIP-2, and TNF-α, and transient eosinophilia with increased levels of IL-13 and eotaxin-1 (from 2 to 6 wk). YM1, YM2, and acidic mammalian chitinase, all associated with Th2-type inflammation in asthma and helmintic infection (4–7), are also elevated in *Scnn1b*-Tg mice. Moreover, *Scnn1b*-Tg mice exhibit transient and spotty necrotic degeneration of Clara cells in the intrapulmonary airways, peaking at day 3 and being completely resolved by day 10, and early neonatal air-trapping that later results in emphysematous changes (3). As surviving *Scnn1b*-Tg mice age, lymphocytic aggregates similar to those described in the lungs of COPD patients (8) become more frequent, suggesting progressive development of

*Cystic Fibrosis/Pulmonary Research and Treatment Center, The University of North Carolina at Chapel Hill, Chapel Hill, NC, 27599; and †Department of Pediatrics III, Pediatric Pulmonology and Cystic Fibrosis Center, University of Heidelberg, Heidelberg, Germany

Received for publication August 5, 2008. Accepted for publication January 21, 2009.

The costs of publication of this article were defrayed in part by the payment of page charges. This article must therefore be hereby marked *advertisement* in accordance with 18 U.S.C. Section 1734 solely to indicate this fact.

[1] This work was funded by North American Cystic Fibrosis Foundation (CFF) Grant LIVRAG04I0 (to A.L.), Deutsche Forschungsgemeinschaft MA2081/2-1 grant (to M.A.M.), National Institutes of Health (NIH) Grant P30 DK065988 and CFF grant R026-CR02 (to W.K.O.), NIH Grants P50 HL060280, P01 HL034322, P30 DK065988, and P50 HL084934 (to R.C.B.), and CFF Grant RANDEL07P0 (to S.H.R.).

[2] Address correspondence and reprint requests to Dr. Alessandra Livraghi, Cystic Fibrosis/Pulmonary Research and Treatment Center, University of North Carolina at Chapel Hill, CB 7248 Thurston Bowles Building, Room 6029, Chapel Hill, NC 27599. E-mail address: alessandra_livraghi@med.unc.edu

[3] Abbreviations used in this paper: CCSP, Clara cell secretory protein; Tg, transgenic; ASL, airway surface liquid; CF, cystic fibrosis; CB, chronic bronchitis; COPD, chronic obstructive pulmonary disease; MuSC, mucous secretory cells; BAL, bronchoalveolar lavage; WT, wild type; KO, knockout; BALF, bronchoalveolar lavage fluid; AB/PAS, Alcian blue/periodic acid-Schiff; Scnn1b, sodium channel nonvoltage gated 1, β subunit.

www.jimmunol.org/cgi/doi/10.4049/jimmunol.0802557

adaptive immune responses (9). Collectively, the presence of MuSC metaplasia, airspace enlargement, and inflammatory markers of both Th1- and Th2-type responses suggests that the mucosal immune response in *Scnn1b*-Tg mice is multifactorial and shares features of both aerotoxin- and allergen-mediated lung pathologies, such as COPD and asthma.

One strategy to identify key signaling pathways in the development of lung pathology is to crossbreed *Scnn1b*-Tg mice to mice deficient in putatively relevant inflammatory mediators. Based on the *Scnn1b*-Tg mouse phenotype, we focused our studies on two pathways, namely TNF-α and IL-4Rα. Exogenous administration or transgenic overexpression of TNF-α in murine airways promotes mucus secretion, lymphoid hyperplasia, and emphysema (10–13). Conversely, genetic ablation of TNF-α-mediated signaling prevents cigarette smoke-induced matrix breakdown, macrophage and neutrophil influx, and late-onset emphysema (14). IL-4Rα is a shared component of the receptors for IL-4 and IL-13, two cytokines that trigger Th2-type airway inflammation and remodeling (15, 16) and have been highly implicated in the pathogenesis of allergy and asthma (17, 18). Ablation of IL-4Rα signaling has been shown to suppress IL-4- and IL-13-induced airway MuSC metaplasia and eosinophilic inflammation (19) and inhibit accumulation of chitinases YM1/2 in bronchoalveolar lavage (BAL) of allergic mice (20). In particular, Clara cell-targeted deletion of IL-4Rα was sufficient to prevent allergen-induced MuSC metaplasia (21). Finally, in vitro studies showed that both TNF-α (22–24) and IL-4/IL-13 (25) inhibited ENaC-mediated Na^+ absorption and could thus modify the *Scnn1b*-Tg mouse phenotype.

To study the contribution of TNF-α and IL-4Rα signaling to the development of *Scnn1b*-Tg mouse lung pathology, we crossbred *Scnn1b*-Tg mice with mice deficient in TNF-α, TNF-αR1, or IL-4Rα and studied survival, lung pathology, BAL cell, cytokine/chemokine, and mucin content, and airway ion transport properties. As a complementary approach to our genetic studies, we tested whether established *Scnn1b*-Tg mouse lung disease was modulated by pharmacologic treatment with prednisolone, a broad spectrum antiinflammatory glucocorticoid (26) shown to reduce eosinophilia and MuSC metaplasia in murine models of atopic asthma (27–31).

Materials and Methods

Mice

All mice were housed in individually ventilated microisolator cages, in a specific pathogen-free facility maintained at the University of North Carolina at Chapel Hill, on a 12-h day/night cycle. They were fed a regular chow diet and given water ad libitum. Hemizygous *Scnn1b*-Tg mice (*Scnn1b*-Tg$^{+/-}$, or *Scnn1b*-Tg) and littermate controls (*Scnn1b*-Tg negative, or wild type (WT)) were obtained by breeding *Scnn1b*-Tg mice with C3H/HeN:C57BL6/N (C3:B6) F_1 mice (Taconic) and genotyped for *Scnn1b*-Tg expression by PCR of genomic DNA, as originally described (1). To generate *Scnn1b*-Tg/IL-4Rα-deficient mice and appropriate littermate controls, we first bred *Scnn1b*-Tg mice with IL-4Rα knockout (KO) mice (IL-4R$\alpha^{-/-}$, strain BALB/c-*Il4ra*^{tm1Sz}/J (32), kindly provided to us by Dr. Beverly Koller, University of North Carolina at Chapel Hill; IL-4Rα-deficient mice exhibit loss of IL-4- and IL-13-mediated responses upon challenge, but they do not exhibit phenotypic abnormalities at baseline (32)) and generated IL-4Rα heterozygous (IL-4R$\alpha^{+/-}$) *Scnn1b*-Tg mice. IL-4R$\alpha^{+/-}$ *Scnn1b*-Tg mice were then bred with IL-4Rα KO mice to obtain experimental animals of four predicted genotypes: IL-4R$\alpha^{+/-}$, WT; IL-4R$\alpha^{-/-}$, WT; IL-4R$\alpha^{+/-}$, *Scnn1b*-Tg; and IL-4R$\alpha^{-/-}$, *Scnn1b*-Tg. We note that this breeding strategy generated control mice heterozygous for the deleted gene of interest, which were not expected to be different from homozygous WT mice. However, we gained the advantage that experimental animals of all four genotypes, with the expected Mendelian distribution of 25% each, shared the identical environment (i.e., littermate controls). We used multiple breeders and multiple litters per breeder to minimize founder and litter order effects. Although nonrandom strain effects can never be ruled out, the use of littermate controls is the best possible approach for reducing the chance of misinterpreting transgene or knockout effects (33). The same breeding strategy was used to generate experimental animals for the TNF-α KO $\times$ *Scnn1b*-Tg and TNF-αR1 KO $\times$ *Scnn1b*-Tg crosses, with the exception that we used inbred C57BL6/N *Scnn1b*-Tg mice, recently generated by backcrossing the original C3:B6 *Scnn1b*-Tg mouse (line 6608) with C57BL/6N inbred mice for 12 generations (9). Both TNF-α KO (B6;129-*Tnf*^{tm1Gkl}/J (34), mixed 129S/SvEv:C57BL/6J background, stock 003008) and TNF-αR1 KO (B6.129-*Tnfrsf1a*^{tm1Mak}/J (35), C57BL/6J background, stock 002818) mice were from The Jackson Laboratory. WT inbred C57BL/6N, C3H/HeN, and BALB/cJ mice for studies of normal neonatal development were obtained from The Jackson Laboratory and Taconic. For prednisolone treatment experiments, we used inbred C57BL6/N *Scnn1b*-Tg mice and their WT littermates. All animal studies were approved by the Institutional Animal Care and Use Committee of the University of North Carolina at Chapel Hill and performed according to the principles outlined by the Animal Welfare and the National Institutes of Health guidelines for the care and use of animals in biomedical research.

Prednisolone treatment

Weaned 5- to 6-wk-old C57BL/6N *Scnn1b*-Tg mice and WT littermates were administered prednisolone (20 mg/kg/day) by i.p. injection, for 2 wk. Prednisolone (provided by Pfizer) was administered twice a day, that is, two injections of 10 mg/kg in 100 μl of sterile vehicle (0.1% Pluronic P105 in sterile, pyrogen-free 150 mM NaCl plus 10% DMSO), ~10 h apart. Control mice (not receiving prednisolone) were injected with 100 μl of vehicle on the same schedule. Mice were weighed every day before each injection. At the end of the 2 wk treatment, BAL was performed and lung tissue harvested for histological evaluation of lung pathology, as described below.

Bronchoalveolar lavage

For 10-day-old or older mice, we used a standardized procedure to obtain both BAL cell counts and lung histology from each animal. Mice were euthanized by exsanguination under deep avertin (2,2,2-tribromoethanol) anesthesia and the chest cavity was opened to ligate the left main bronchus. A blunt needle (20-gauge for adults, 22-gauge for 5- to 10-day-old pups) was inserted through a small incision in the upper trachea and tied in place with 3.0 silk. After ligation of the left main stem bronchus, BAL was performed on the right lobes by instilling a volume of room temperature, sterile PBS determined by the formula: (mouse weight (g) $\times$ 0.0175 ml = ml PBS instilled) (36). Due to their small size, 5-day-old pups were subject to either whole lung lavage (mouse weight (g) $\times$ 0.035 ml = ml PBS instilled) or fixation for histology, but not both. BAL was performed by gently injecting and retrieving the PBS volume three times. This procedure was conducted a second time with an equal volume of PBS, and fractions were pooled. Return volume was consistently >80% of the instilled volume. BAL cells were pelleted by centrifugation at 1000 $\times$ *g* for 5 min at 4°C and the cell-free supernatant (BAL fluid, or BALF) was collected and stored at −80°C for further analysis. BAL cells were resuspended in 100 μl of PBS and total cells were counted with a hemocytometer. Cytospin slides of 30,000–60,000 cells/slide were obtained (StatSpin CytoFuge 2), air dried, and stained with modified Giemsa for differential cell counts (Newcomer Supply) of at least 200 cells per slide. After BAL, the left bronchial ligature was removed and the left lung was immersion-fixed in 10% neutral-buffered formalin to prevent dislodging of airway luminal contents.

Lung histology

Fixed lungs were embedded in paraffin oriented to maximize longitudinal sectioning of primary bronchi, sectioned to a thickness of 4–6 μm, and stained with H&E for assessment of lung morphology and Alcian blue/periodic acid-Schiff staining (AB/PAS) for mucopolysaccharides. The severity of lung pathology was graded semiquantitatively on a scale ranging from 0 to 3 for the following features: 1) airway obstruction, that is, airways obstructed by AB/PAS-positive mucus: 0, no obstruction; 1, one airway partially or totally obstructed; 2, two airways partially or totally obstructed; 3, three or more airways partially or totally obstructed; 2) MuSC abundance, that is, estimated percentage of AB/PAS positive cells in airway epithelium: 0, none; 1, 0–5% MuSC; 2, 5–20% MuSC; 3, ≥20% MuSC; 3) airspace enlargement, that is, enlargement of the alveoli in the parenchymal space: 0, none; 1, spotty; 2, 50% of parenchyma; 3, >50% of parenchyma; 4) lymphoid hyperplasia, that is, perivascular, peribronchial, or parenchymal lymphoid aggregates: 0, none; 1, one nodule per lung section; 2, two nodules per lung section; 3, three or more nodules per lung section; and 5) airway inflammation, that is, interstitial thickening and inflammatory cell infiltrate: 1, one airway; 2, two airways; 3, three or more

airways. To confirm the results of the semiquantitative score for MuSC abundance, we used MetaMorph image analysis software (MDS Analytical Technologies) and determined the percentage of airway epithelial area positive for AB/PAS staining. Briefly, three random fields within the left lung proximal main stem bronchus were photographed with an upright Nikon Microphot-SA microscope interfaced with a DXM 1200 color camera (Nikon Instruments) at ×20 magnification. The AB/PAS-positive area was measured by thresholding and was divided by the total epithelial area, to give the volume density of stored mucosubstances. Tissue blocks received a numerical code at time of embedding, and scoring of the slides was performed by an investigator blinded to specimen genotype.

Agarose gel mucin Western blot

This method was used to measure secreted mucins, as described in detail (37). BAL samples were centrifuged at low speed (1000 × *g* for 5 min). Total protein concentration of BALF was determined using the Microplate BCA protein assay, according to the manufacturer's instructions (Thermo Scientific), and was used to control for equivalent loading, since the large molecular sieve of agarose gels does not allow retention of globular proteins conventionally used for normalization. An equal volume of 8 M guanidine hydrochloride (GuHCl) was added to the BALF. GuHCl-dispersed samples were dialyzed against 6 M urea, reduced with 10 mM DTT, and alkylated with 25 mM iodoacetamide. Alternatively, BALF was directly diluted 1/5 in 6 M urea plus 0.1% SDS, reduced, and alkylated. Equal volumes of reduced samples (20–25 μl) were run on 1% agarose gel using a submerged gel electrophoresis apparatus with Tris acetate-EDTA/SDS buffer, at 80 V for 90–120 min. Gels were vacuum-blotted onto nitrocellulose membranes, blocked with Odyssey blocking buffer (OBB; LI-COR Biosciences), and probed with a rabbit polyclonal Ab raised against purified cervical mucins ("reduced subunit antibody", described in Refs. 38, 39). This Ab recognizes the cysteine-rich domain of almost all mucins and is thus a "pan-mucin" detection reagent. Alternatively, blots were probed with a rabbit polyclonal Ab against murine Muc-5b (described in Refs. 40, 41). Pan-mucin and Muc5b Abs were diluted 1/2000 and 1/1000 in OBB plus 0.1% Tween 20 (OBBT), respectively. The secondary Ab was Alexa Fluor 680 goat anti-rabbit IgG, diluted 1/15,000 in OBBT. Detection and analysis of specific signals were performed using the Odyssey infrared imaging system (LI-COR Biosciences).

Measurement of cytokines and chemokines in BALF

Aliquots of cell-free BALF, stored at −80°C, were used to measure mouse TNF-α, KC, IL-4, IL-5, IL-13, IL-17, MCP-1, IL-6, MIP-2, and INFγ using a bead-based assay (Upstate (Millipore) Beadlyte multiplex assays/Luminex), according to the manufacturer's instructions.

Ussing chamber measurements of airway bioelectric properties

Freshly excised tracheas were mounted in Ussing chambers and equilibrated as described (42). After recording the basal short-circuit current (I_{sc}), the following drugs were added sequentially to the chambers: amiloride (10^{-4} M, apical), forskolin (10^{-5} M, apical), UTP (10^{-4} M, apical), and bumetanide (10^{-4} M, basolateral), and changes in I_{sc} were recorded.

Statistical analyses

Statistical analyses were performed using SigmaStat 3.1 or GraphPad Prism 4.0. Survival curves were compared using Kaplan-Meier log rank analysis and Holm-Sidak multiple comparison. One-way ANOVA followed by Tukey's post hoc test for multiple comparisons were used to determine significant differences among groups. A p value of <0.05 was considered statistically significant. All data are expressed as means ± SEM.

Results

TNF-α signaling is not essential for airway inflammation and remodeling in Scnn1b-*Tg mice*

To investigate the role of TNF-α in airway inflammation and remodeling in *Scnn1b*-Tg mice, we crossbred *Scnn1b*-Tg mice (inbred line C57BL/6N) with mice lacking either TNF-α ligand (TNF-$\alpha^{-/-}$ mouse, C57:129Sv mixed background) or TNF-αR1 (TNF-αR1$^{-/-}$ mouse, C57BL/6J background), and produced four possible genotypes as described in *Materials and Methods*. Both crosses gave similar results, and data for the TNF-α KO cross are shown in Fig. 1 and in supplemental Fig. 1, *D* and *E*,[4] while data for the TNF-αR1 KO cross are provided in supplemental Fig. 1*A–C*.

Lack of TNF-α or TNF-αR1 did not alter survival of *Scnn1b*-Tg mice, and all mice had comparable, high survival, ranging between 80 and 95% (Fig. 1*A* and supplemental Fig. 1*A*). Survival of *Scnn1b*-Tg mice differed from previously published studies (1), likely due to strain differences. In fact, ongoing backcross studies in our laboratory, aimed at obtaining inbred strains of *Scnn1b*-Tg mice, have shown that survival is significantly increased in the C57BL/6N and 129S1/SvImJ backgrounds (9) compared with the original mixed C3:B6 background (1).

TNF-α was significantly elevated in BAL from TNF-$\alpha^{+/-}$ *Scnn1b*-Tg mice in comparison to TNF-$\alpha^{+/-}$ WT littermates (Fig. 1*B*, *left panel*), consistent with previous reports (3). As expected due to TNF-α gene deletion, TNF-α was undetectable in BAL samples from TNF-$\alpha^{-/-}$ *Scnn1b*-Tg mice. KC was significantly elevated in both TNF-$\alpha^{-/-}$ *Scnn1b*-Tg mice and TNF-$\alpha^{+/-}$ *Scnn1b*-Tg mice (Fig. 1*B*, *right panel*), indicating that absence of TNF-α did not impact the production of this neutrophil chemoattractant.

Histological lesions typically observed in *Scnn1b*-Tg mice are illustrated in Fig. 1*C*. Semiquantitative scoring of these lesions in 5-wk-old mice from the TNF-α KO × *Scnn1b*-Tg cross revealed significant mucus plugging, airspace enlargement, lymphoid hyperplasia, and airway inflammation in *Scnn1b*-Tg mice compared with WT littermates, irrespective of TNF-α or TNF-αR1 status (Fig. 1*D* and supplemental Fig. 1*B*). TNF-α or TNF-αR1 deficiency did not alter lung histology in WT mice. Absence of TNF-α or TNF-αR1 did not prevent neutrophil and eosinophil infiltration in *Scnn1b*-Tg mouse lung, as assessed by BAL differential cell counts (Fig. 1*E* and supplemental Fig. 1*C*). Large, foamy alveolar macrophages (see Fig. 1*C10*) were present in both TNF-α-sufficient and -deficient *Scnn1b*-Tg mice. Furthermore, TNF-α ablation did not affect lung histopathology or BAL differential cell counts in 10-day-old *Scnn1b*-Tg or WT mice (supplemental Fig. 1, *D* and *E*).

TNF-α has been shown to down-regulate ENaC activity in airway epithelial cells in vitro (22–24). To test whether lack of TNF-α altered Na^+ transport, we studied freshly excised tracheas from 5-wk-old mice in Ussing chambers (Fig. 1*F*). Amiloride-sensitive short-circuit current (I_{sc}) was significantly greater in *Scnn1b*-Tg mice than in WT mice, consistent with increased ENaC activity and as previously reported (1), but it was not affected by TNF-α status. Collectively, these data indicate that TNF-α or TNFR1 are not essential for development of airway and lung pathology in *Scnn1b*-Tg mice.

Absence of IL-4Rα enhances neonatal survival in Scnn1b-*Tg mice*

To determine the role of IL-4Rα signaling in the development of *Scnn1b*-Tg mouse lung pathology, we crossed *Scnn1b*-Tg (mixed C3:B6 background) and IL-4Rα KO mice (IL-4Rα KO, BALB/cJ background), as described in *Materials and Methods*. As expected, the survival of WT mice was high (100%) and was unaffected by the absence of IL-4Rα. In contrast, *Scnn1b*-Tg mice exhibited characteristic early postnatal mortality (Fig. 2*A*). In agreement with our backcross studies, introduction of the BALB/cJ background reduced *Scnn1b*-Tg mouse survival in comparison to the mixed C3:B6 background (32% vs 50% for C3:B6:BALB and C3:B6 (1), respectively). However, genetic ablation of IL-4Rα significantly increased survival of *Scnn1b*-Tg mice (54% vs 32% for

[4] The online version of this article contains supplemental material.

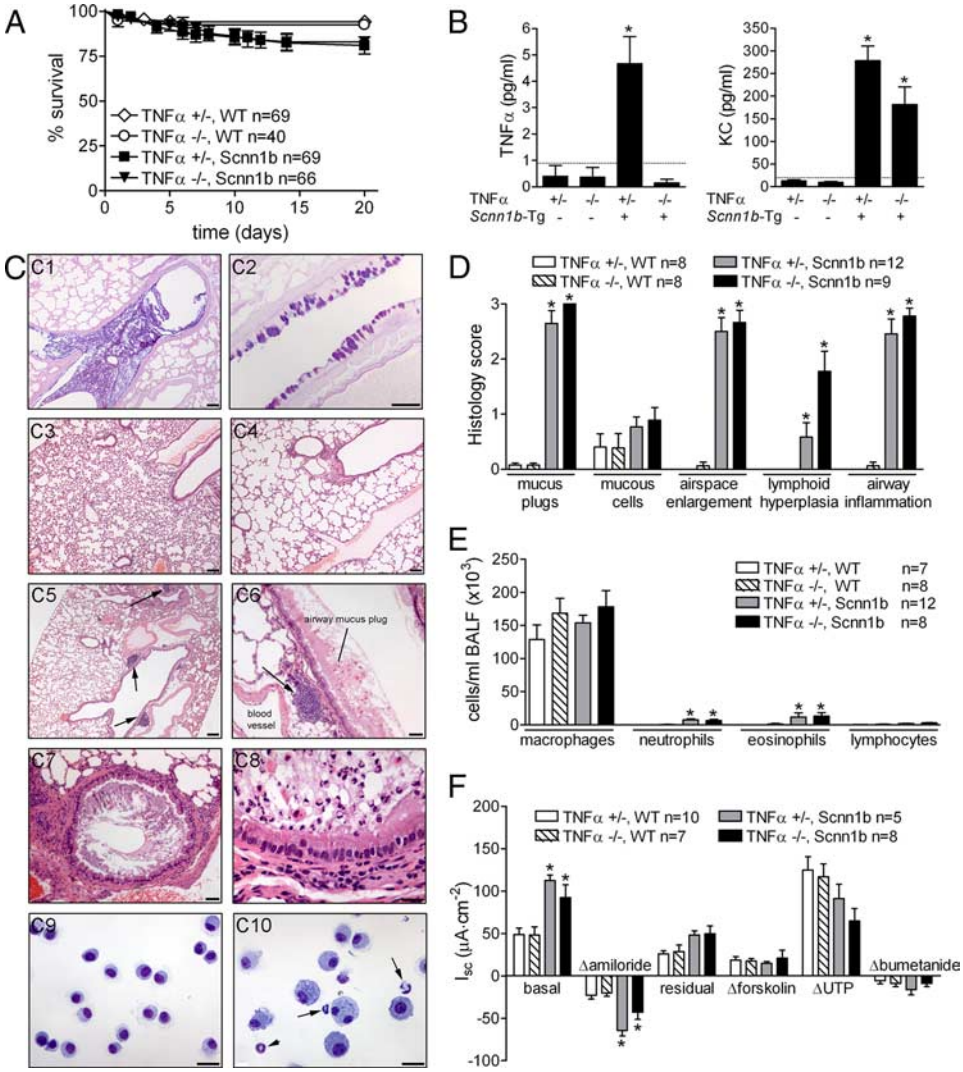

FIGURE 1. Minimal effect of TNF-α deletion on the *Scnn1b*-Tg mouse phenotype. *A*, Survival curves. Introduction of the 129S/SvEv:C57BL/6J background (TNF-α KO) decreases mortality of *Scnn1b*-Tg mice compared with the original C3H/HeN:C57BL/6N strain, irrespective of TNF-α status. See text for details. *B*, BAL cytokine/chemokine profile in 5-wk-old mice. *, $p < 0.05$ vs TNF-$\alpha^{+/-}$ WT mice. The dotted line represents the assay lower detection limit. *C*, Representative photomicrographs illustrating characteristic lesions in 5-wk-old TNF-$\alpha^{-/-}$ *Scnn1b*-Tg mice. H&E stain unless indicated. *1*, Mucus plugs, AB/PAS stain, scale bar = 100 μm. *2*, Mucous secretory cells, AB/PAS stain, scale bar = 50 μm. *3* and *4*, Distal airspace enlargement, comparing WT (*3*) and *Scnn1b*-Tg mice (*4*), scale bar = 200 μm. *5* and *6*, Lymphoid hyperplasia, at low (*5*, scale bar = 200 μm) and high (*6*, scale bar = 50 μm) magnification. *7* and *8*, Airway inflammation, at low (*7*, scale bar = 50 μm) and high (*8*, scale bar = 20 μm) magnification. Cytospins from WT (*9*) and *Scnn1b*-Tg mice (*10*), illustrating large/foamy macrophages, neutrophils (arrows), and eosinophils (arrowhead), Giemsa stain, scale bar = 20 μm. *D*, Semiquantitative histopathology scores indicating similar lesions in TNF-$\alpha^{+/-}$ and TNF-$\alpha^{-/-}$ *Scnn1b*-Tg mice. *, $p < 0.05$ vs TNF-$\alpha^{+/-}$ WT mice. *E*, Differential BAL cell counts. *, $p < 0.05$ vs TNF-$\alpha^{+/-}$ WT mice. *F*, Ion transport properties of freshly excised tracheal tissues. "Basal" indicates the I_{sc} before drug application. The change in I_{sc} (Δ) after sequential drug addition is shown. "Residual" I_{sc} is the I_{sc} remaining after amiloride application. *, $p < 0.05$ vs TNF-$\alpha^{+/-}$ WT mice.

IL-4R$\alpha^{-/-}$ *Scnn1b*-Tg vs IL-4R$\alpha^{+/-}$ *Scnn1b*-Tg mice; Fig. 2*A*). By genotyping pups at days 1–3, we verified that all four genotypes were present in the expected Mendelian proportions at birth (supplemental Fig. 2*A*). The improvement in survival occurred between 5 and 12 days, the window of peak mortality for *Scnn1b*-Tg mice, and stabilized thereafter (Fig. 2*A*).

Absence of IL-4Rα decreases neonatal MuSC abundance and eosinophilia in WT and Scnn1b-*Tg mice*

To elucidate the reason(s) for improved survival in IL-4Rα-deficient *Scnn1b*-Tg mice, we examined lung histology and BAL cell counts in 10-day-old pups. Although MuSC are rare in adult WT unchallenged mice, we detected luminal mucus and rather abundant MuSC in the bronchi of 10-day-old IL-4R$\alpha^{+/-}$ WT mice (Fig. 2, *B3* and *C*). However, both mucus and MuSC were virtually absent in IL-4R$\alpha^{-/-}$ WT mice (Fig. 2, *B4* and *C*). Although bronchial mucus plugging, as detected histologically, was similar in both IL-4Rα-sufficient and -deficient *Scnn1b*-Tg mice (Fig. 2*C*), MuSC were significantly reduced in IL-4Rα-deficient *Scnn1b*-Tg mice (Fig. 2, *B7*, *B8*, and *C*), which was confirmed by computer image analysis of AB/PAS-positive stored mucosubstances (supplemental Fig. 2*B*). However, absence of IL-4Rα did not ameliorate the parenchymal air space enlargement and airway inflammatory lesions already evident in young *Scnn1b*-Tg mice (Fig. 2*C*). Lymphoid hyperplasia was never observed in 10-day-old animals.

Absence of IL-4Rα decreased BAL eosinophils in 10-day-old *Scnn1b*-Tg mice in comparison to IL-4R$\alpha^{+/-}$ *Scnn1b*-Tg mice (Fig. 2*D*), but failed to reduce the pronounced macrophage and

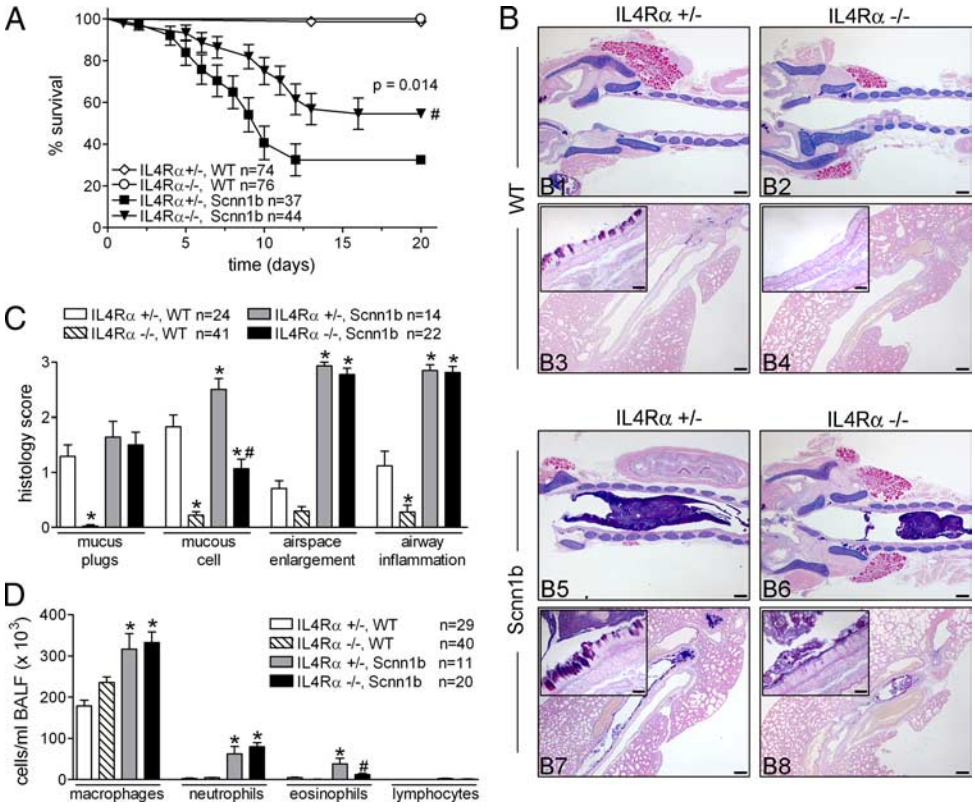

FIGURE 2. Genetic deletion of IL-4Rα improves neonatal survival and decreases mucous secretory cells and eosinophils in 10-day-old *Scnn1b*-Tg mice. *A*, Survival curves. Introduction of the BALB/c/J background (IL-4Rα KO) increases mortality of *Scnn1b*-Tg mice compared with the original C3H/HeN: C57BL/6N strain, and absence of IL-4Rα improved survival. See text for details. #, $p = 0.014$ vs IL-4Rα$^{+/-}$ *Scnn1b*-Tg mice. *B*, Representative photomicrographs of trachea (*1* and *2* for WT and *5* and *6* for *Scnn1b*-Tg mice) and lung (*3* and *4* for WT and *7* and *8* for *Scnn1b*-Tg mice) of IL-4Rα$^{+/-}$ and IL-4Rα$^{-/-}$ mice, AB/PAS stain. Scale bars: low magnification = 200 μm, high magnification insets = 20 μm. *C*, Semiquantitative histopathology scores. ∗, $p < 0.05$ vs IL-4Rα$^{+/-}$ WT mice. #, $p < 0.05$ vs IL-4Rα$^{+/-}$ *Scnn1b*-Tg mice. *D*, Differential BAL cell counts. ∗, $p < 0.05$ vs IL-4Rα$^{+/-}$ WT mice. #, $p < 0.05$ vs IL-4Rα$^{+/-}$ *Scnn1b*-Tg mice.

neutrophil infiltrate. Low, but readily detectable numbers of eosinophils were also present in BAL from 10-day-old IL-4Rα$^{+/-}$ WT mice (4890 ± 100 cells/ml), which was reduced in IL-4Rα$^{-/-}$ WT mice (900 ± 260 cells/ml).

Similar to the results we obtained for genetic deletion of TNF-α, we did not detect changes in airway ion transport properties of either WT or *Scnn1b*-Tg mice due to the absence of IL-4Rα (supplemental Fig. 2*C*).

Absence of IL-4Rα does not mitigate chronic lung pathology in surviving adult Scnn1b-*Tg mice*

We next tested whether absence of IL-4Rα modified chronic lung pathology or inflammation in surviving 5-wk-old *Scnn1b*-Tg mice. As expected, no differences were detected in adult WT mice due to the presence or absence of IL-4Rα (Fig. 3, *A1* and *A2*). Absence of IL-4Rα minimally altered lung histology scores and BAL parameters in adult *Scnn1b*-Tg mice. Specifically, airway mucus plugging, MuSC abundance, air space enlargement, lymphoid hyperplasia, and airway inflammation were equivalent in IL-4Rα-deficient and -sufficient *Scnn1b*-Tg mice (Fig. 3, *A3*, *A4*, and *B*). As seen in 10-day-old animals, BAL eosinophils were reduced in IL-4Rα$^{-/-}$ *Scnn1b*-Tg mice in comparison to IL-4Rα-sufficient mice, but marked neutrophilia persisted in *Scnn1b*-Tg mice regardless of IL-4Rα status (Fig. 3*C*).

Absence of IL-4Rα does not modify the BAL inflammatory mediator profile of neonatal or adult Scnn1b-*Tg mice*

Genetic deletion of IL-4Rα reduced neonatal MuSC and improved survival in *Scnn1b*-Tg mice, but it did not eliminate chronic neutrophilic inflammation. To elucidate the IL-4Rα-independent mechanisms driving the development of chronic lung pathology, we analyzed BALF cytokines in 10-day-old and 5-wk-old *Scnn1b*-Tg mice. INFγ, MCP-1, and IL-17 were below the detection limit in all samples. KC and TNF-α levels were elevated in *Scnn1b*-Tg mice compared with WT littermates at both early and late time points and were not altered by IL-4Rα status (Fig. 4, *A* and *B*). A trend toward higher IL-4, IL-5, and IL-13 levels was observed in 10-day-old *Scnn1b*-Tg mice in comparison to WT littermates, which normalized by 5 wk of age (Fig. 4*C–E*; IL-4, 2.0 ± 0.7 vs 0.02 ± 0.02; IL-5, 127 ± 37 vs 15.2 ± 7; IL-13, 17.6 ± 6 vs 4.3 ± 1 pg/ml for 10-day-old *Scnn1b*-Tg and WT mice, respectively; $n = 10$). Absence of IL-4Rα caused a small but significant decrease in IL-5 in 5-wk-old *Scnn1b*-Tg mice. In agreement with a previous study (43), transient eosinophilia in 10-day-old WT mice was not associated with increased BALF levels of IL-4, IL-5, and IL-13 in comparison to adult mice.

Elements of Scnn1b-*Tg airway and lung pathology are glucocorticoid resistant*

In view of the minimal impact of TNF-α, TNFR1, or IL-4Rα genetic removal on adult *Scnn1b*-Tg mouse lung pathology/inflammation, we investigated the effects of glucocorticoid treatment. Daily systemic administration of 20 mg/kg prednisolone for 2 wk, starting at 5–6 wk of age, inhibited the body weight gain (2.5 g/week) typical of both *Scnn1b*-Tg and WT littermates (supplemental Fig. 3, *A* and *B*), likely reflecting catabolic effects of high-dose systemic glucocorticoids (48) and indicating effective drug delivery. Prednisolone administration markedly diminished MuSC abundance and eosinophilia and significantly reduced the incidence of lymphoid aggregates in *Scnn1b*-Tg mice, but it failed to ameliorate mucus plugging, airway inflammation, and neutrophilia (Fig. 5*A–C*). BAL lymphocyte counts were decreased by prednisolone, but not significantly (2620 ± 867 and 993 ± 580 lymphocytes/ml BAL for vehicle and prednisolone, respectively). In *Scnn1b*-Tg mice, prednisolone administration increased the BALF total protein content (Fig. 5*D*), but it did not affect the levels of KC, MIP-2, TNF-α, and IL-6, which were significantly elevated in comparison to WT littermates (data not shown). Interestingly,

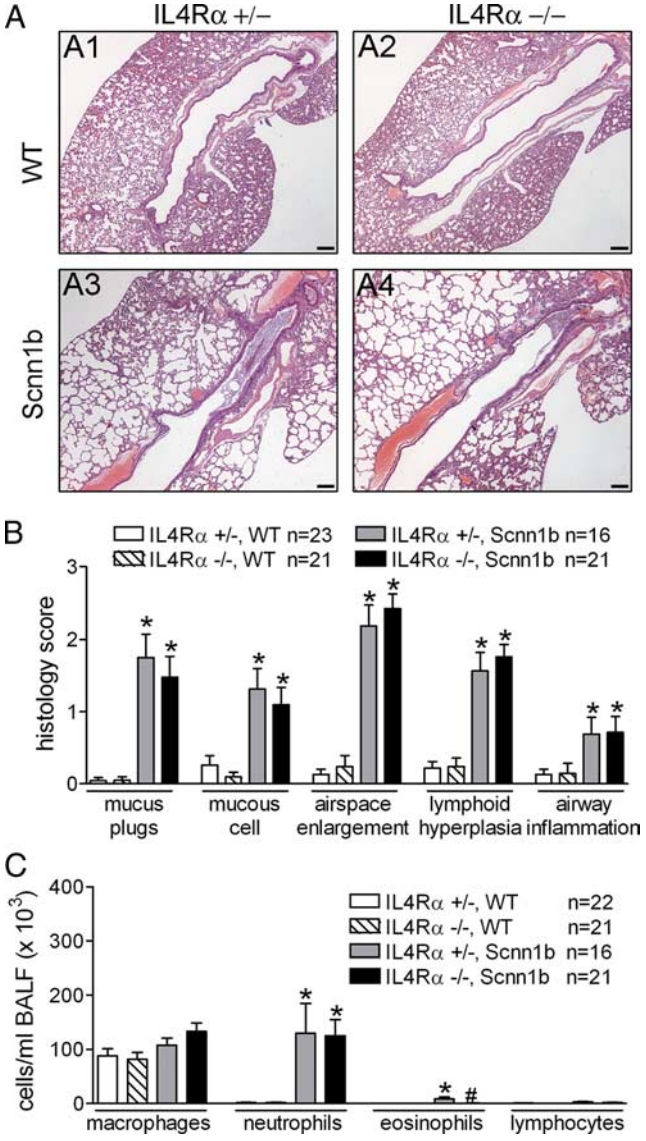

FIGURE 3. Minimal effect of IL-4Rα deletion on the adult *Scnn1b*-Tg mouse phenotype. *A*, Representative photomicrographs of lung histology in WT (*1* and *2*) and *Scnn1b*-Tg (*3* and *4*) mice, H&E stain, scale bar = 200 μm. *B*, Semiquantitative histopathology scores. *, $p < 0.05$ vs IL-4Rα$^{+/-}$ WT mice. *C*, Differential BAL cell counts. *, $p < 0.05$ vs IL-4Rα$^{+/-}$ WT mice. #, $p < 0.05$ vs IL-4Rα$^{+/-}$ *Scnn1b*-Tg mice.

prednisolone also reduced the normal abundance of bronchial MuSC in WT mice (Fig. 5, *A* and *B2*). We assessed whether the prednisolone-induced reduction in MuSC correlated with decreased BAL mucin protein content, as assessed by agarose gel Western blots. As shown in Fig. 5*E*, BAL mucin content was significantly higher in *Scnn1b*-Tg mice compared with WT mice, and it was not reduced as a function of prednisolone administration.

Normal postnatal development of mouse airways entails a spatially and temporally confined abundance of MuSC and transient eosinophilia

The presence of AB/PAS-positive MuSC and eosinophils in the airways of 10-day-old IL-4Rα-sufficient WT mice and their absence in IL-4Rα-deficient mice prompted us to investigate whether the appearance of MuSC and eosinophils was a normal developmental feature of the mouse respiratory system. We analyzed tracheal and lung histology in 5-day-old, 10-day-old, and 5-wk-old mice from C57BL/6N, C3H/HeN, and BALB/cJ inbred strains and found a distinct developmental pattern. At day 5, when submucosal glands are rudimentary (44, 45), AB/PAS-positive cells were abundant in the trachea (illustrated for the C57BL/6N strain in Fig. 6*A1*) and absent in the bronchi (Fig. 6*A4*), whereas by day 10 their frequency diminished in the trachea (Fig. 6*A2*) and increased in the proximal portion of the main stem bronchi (Fig. 6*A5*). At 5 wk, MuSC were virtually absent in the trachea (Fig. 6*A3*), and the number of bronchial MuSC stabilized at the low levels found in adult mice (Fig. 6*A6*). This pattern was conserved among inbred strains (Fig. 6*B* for C57BL/6N and supplemental Fig. 4, *A* and *B*, for C3H/HeN and BALB/cJ).

BAL differential cell counts from 5-day-old, 10-day-old, and 5-wk-old C57BL/6N, C3H/HeN, and BALB/cJ mice revealed mainly macrophages, although we detected rare neutrophils in 5- to 10-day-old mice, which were absent in adult animals (Fig. 6*C* for C57BL/6N and supplemental Fig. 4, *C* and *D*, for C3H/HeN and BALB/cJ). Notably, we also found a subtle but consistent degree of eosinophilia in 10 day-old C57BL/6N and C3H/HeN mice. Eosinophil counts were significantly lower in 10 day-old BALB/cJ mice (supplemental Fig. 4*D*) compared with C57BL/6N and C3H/HeN mice, which is consistent with previous studies comparing allergic BALB/cJ and C57BL/6N mice and the reported lower affinity of the BALB/c IL-4Rα variant for IL-4 (46, 47).

BAL secreted mucin content is increased in Scnn1b-*Tg mice*

To test for a biochemical correlate of the time-dependent changes in MuSC observed in WT mice, and to assess how BALF mucin content may be affected by airway surface dehydration, we performed a time-course analysis in WT mice and their *Scnn1b*-Tg

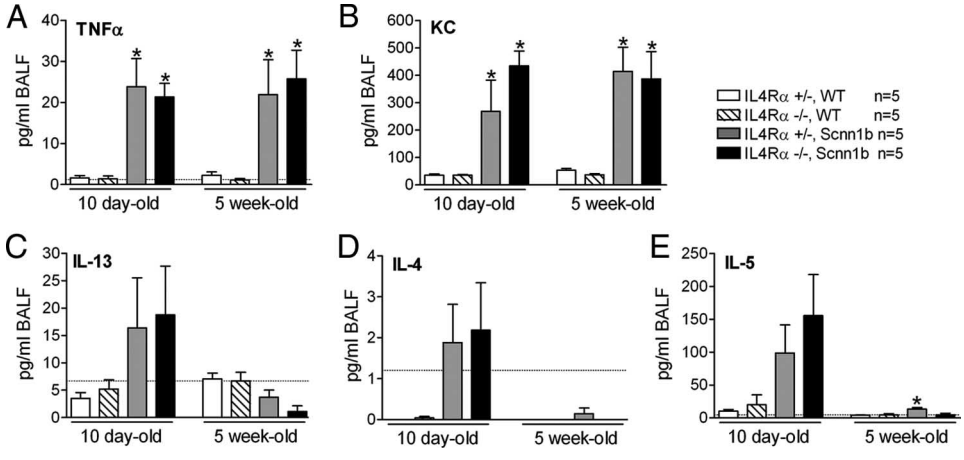

FIGURE 4. IL-4Rα deletion in *Scnn1b*-Tg mice has minimal effect on sustained BAL TNF-α and KC and transient Th-2 cytokines. BAL cytokines in 10-day-old and 5-wk-old mice are shown. The dotted line represents the assay lower detection limit. *, $p < 0.05$ vs age-matched IL-4Rα$^{+/-}$ WT mice.

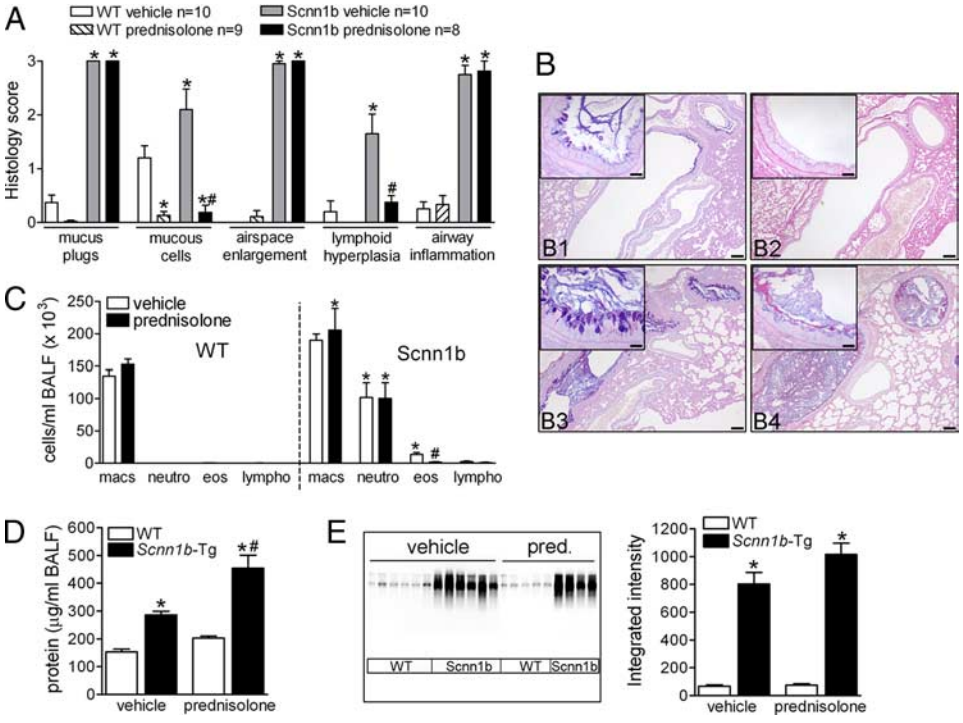

FIGURE 5. Prednisolone treatment of *Scnn1b*-Tg mice reduces MuSC and eosinophils but not neutrophils or BAL mucin content. *A*, Semiquantitative histopathology scores. *, $p < 0.05$ vs vehicle-treated WT mice. #, $p < 0.05$ vs vehicle-treated *Scnn1b*-Tg mice. *B*, Representative photomicrographs of lung sections from WT (*1* and *2*) and *Scnn1b*-Tg mice (*3* and *4*) treated with vehicle (*1* and *3*) or prednisolone (*2* and *4*), AB/PAS stain, scale bars: low magnification = 100 μm, high magnification insets = 20 μm. *C*, BAL differential cell counts. *, $p < 0.05$ vs vehicle-treated WT mice. #, $p < 0.05$ vs vehicle-treated *Scnn1b*-Tg mice. *D*, BALF total protein content. *, $p < 0.05$ vs vehicle-treated WT mice; #, $p < 0.05$ vs vehicle-treated *Scnn1b*-Tg mice. *E*, Agarose gel Western blots and corresponding densitometry of BAL samples from vehicle- and prednisolone-treated mice. Blots were probed with Muc5b Ab. *, $p < 0.05$ vs WT mice.

littermates (C57BL/6N line). At all ages, the BALF mucin content, assessed with Abs that detect either all mucins (Fig. 7*A*) or murine Muc5b (supplemental Fig. 5*A*), were greater in *Scnn1b*-Tg mice than in WT mice, whereas the BALF total protein content for *Scnn1b*-Tg mice was only slightly increased in comparison to WT mice at 5 days and 8 wk of age (Fig. 7*B*). In both WT and *Scnn1b*-Tg littermates, BALF mucins were greatest in 5- and 10-day-old mice and declined in older animals. This temporal pattern of mucin glycoprotein expression is consistent with prior Muc5ac, Muc5b, Muc4, and Gob5 mRNA expression studies (3) and suggests that relative mucin abundance is a consistent feature of neonatal airway development, which is further augmented by impaired mucus clearance in *Scnn1b*-Tg mice. Analysis of BALF mucin content in 5-day-old, 10-day-old, and 5-wk-old

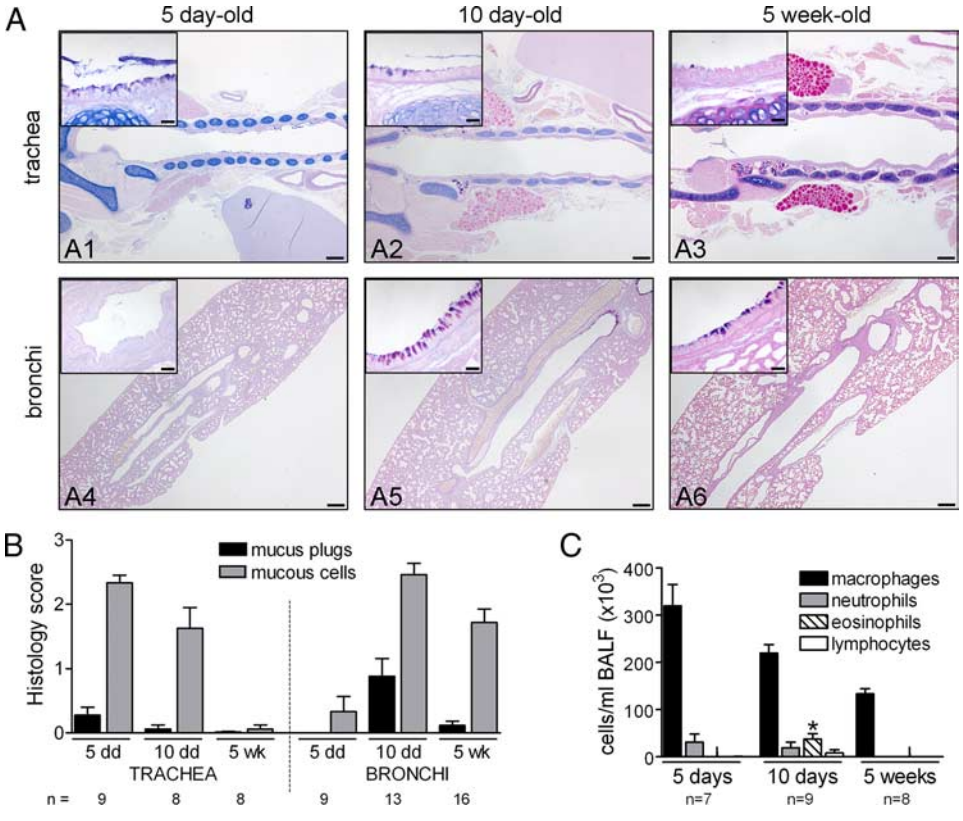

FIGURE 6. MuSC and eosinophils are transiently abundant during normal mouse airway development. *A*, Representative photomicrographs of trachea and bronchi from C57BL/6N mice at age 5 days (*1* and *4*), 10 days (*2* and *5*), and 5 wk (*3* and *6*), AB/PAS stain, scale bars: low magnification = 200 μm, high magnification insets = 20 μm. *B*, Semiquantitative histology scoring of mucus and MuSC in tracheas and bronchi of C57BL/6N mice at age 5 days (5 dd), 10 days (10 dd), and 5 wk. *C*, Differential BAL cell counts in C57BL/6N mice at 5 days, 10 days, and 5 wk of age. *, $p < 0.05$ vs 5-day-old and 5-wk-old mice.

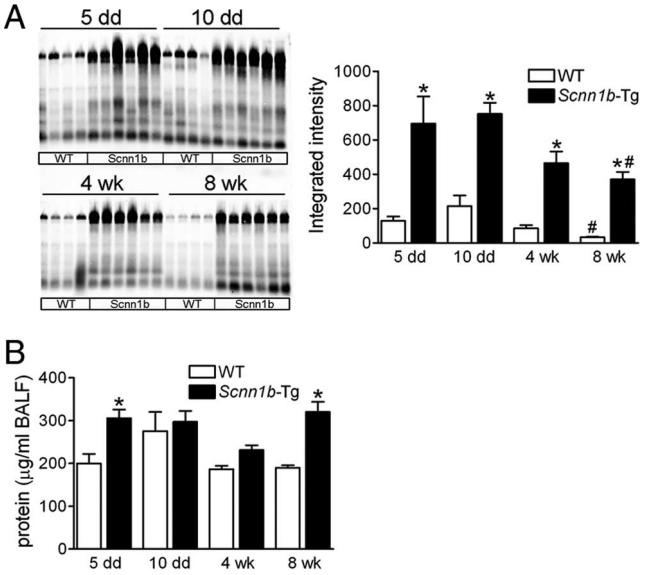

FIGURE 7. BALF total mucin content varies as a function of age and is elevated in neonatal and adult *Scnn1b*-Tg mice. *A*, Agarose gel Western blots and corresponding densitometry of BAL samples from C57BL/6N *Scnn1b*-Tg mice and WT littermates at age 5 days (5 dd), 10 days (10 dd), 4 wk, and 8 wk. Membranes were probed with pan-mucin Ab. ∗, $p < 0.05$ vs WT mice of corresponding age; #, $p < 0.05$ vs 10-day-old mice of corresponding genotype. *B*, BALF total protein content. ∗, $p < 0.05$ vs WT mice of corresponding age.

WT mice of diverse genetic backgrounds (inbred C57BL/6N, C3H/HeN, and BALB/cJ) revealed modest age- and strain-dependent changes in BALF total and Muc5b mucin content (supplemental Fig. 5*B–D*).

Discussion

Adequate airway mucosal surface hydration is essential for effective mucus clearance and lung health. The dynamic progression of lung disease following disruption of mucus clearance in *Scnn1b*-Tg mice suggests a complex host response to airway surface dehydration (3). We investigated the role of TNF-α and IL-4Rα signaling during postnatal lung development and identified aspects of *Scnn1b*-Tg lung pathology that are uniquely susceptible to modification of these pathways and to corticosteroid treatment.

Our studies indicated that TNF-α signaling is not required for triggering or sustaining inflammation, airway remodeling, and distal lung pathology (air space enlargement) in *Scnn1b*-Tg mice. The early appearance of air trapping/airspace enlargement in *Scnn1b*-Tg mice suggests that neonatal airway inflammation might shift the protease/antiprotease balance, impairing alveolarization and generating proinflammatory signals via extracellular matrix degradation, for example, Pro-Gly-Pro peptide (49) and hyaluronan (50). Development of pulmonary lymphoid aggregates in *Scnn1b*-Tg mice was also TNF-α-independent. Since similar nodules are found in lungs of mice repetitively challenged with aerosolized allergen (51, 52) or *Haemophilus influenzae* lysate (53), we speculate that lymphoid hyperplasia is caused by greater and/or more sustained exposure to environmental Ags due to mucus stasis, which in turn enhances adaptive immune responses. Finally, TNF-α inhibits ENaC expression and activity in vitro (22–24) and can down-regulate the rat CCSP promoter (54), which in *Scnn1b*-Tg mice drives βENaC overexpression. However, we found that absence of TNF-α did not alter airway epithelial ion transport properties in excised tracheal tissue from WT or *Scnn1b*-Tg mice, suggesting that TNF-α does not affect either ENaC activity or the CCSP promoter in vivo.

Breeding *Scnn1b*-Tg mice with IL-4Rα gene-deleted mice revealed the existence of IL-4Rα-dependent and -independent elements of *Scnn1b*-Tg mouse lung pathology and provided new insights regarding the role of IL-4Rα signaling during normal neonatal airway development.

In murine models of allergic asthma, eosinophils are involved in collagen deposition and airway smooth muscle hyperplasia, but they are not required for airway hyperreactivity or MuSC metaplasia (55, 56). Our data suggest that eosinophils are not a major determinant of lung pathology in *Scnn1b*-Tg mice. Decreased eosinophils correlated with fewer MuSC in neonatal but not adult IL-4R$\alpha^{-/-}$ *Scnn1b*-Tg mice, and lack of eosinophils did not ameliorate other aspects of lung pathology in *Scnn1b*-Tg mice. Moreover, although a time-dependent role for eosinophils in promoting MuSC abundance is conceivable based on correlations observed between neonatal MuSC and eosinophilia (see Figs. 2, *C* and *D*, 6, *B* and *C*, and supplemental Fig. 4, *A* and *C*), the abundant MuSC found in normal 10-day-old BALB/c/J mice (supplemental Fig. 4*B*), despite the virtual absence of eosinophils (supplemental Fig. 4*D*), suggests that a causal association is unlikely.

The transient and spatially restricted appearance of MuSC in the airways of neonatal WT mice was completely ablated in the absence of IL-4Rα (Fig. 2*C*). We speculate that neonatal MuSC expansion is driven by local, basal levels of Th2 cytokines (IL-4, IL-13, and IL-5; Fig. 4*C–E*), which are difficult to detect once diluted in BAL. In comparison to WT littermates, neonatal *Scnn1b*-Tg mice had higher levels of Th2 cytokines (Fig. 4*C–E*), which likely increased MuSC (Fig. 2*C*). However, absence of IL-4Rα mitigates this response. The residual MuSC in neonatal IL-4R$\alpha^{-/-}$ *Scnn1b*-Tg mice as compared with IL-4R$\alpha^{-/-}$ WT mice (Fig. 2*C*) indicates the existence of an IL-4Rα-independent pathway that triggers MuSC in neonatal *Scnn1b*-Tg mice. Indeed, this pathway could also be active in adult *Scnn1b*-Tg mice, in which MuSC are abundant (Fig. 3*B*) but Th2 cytokine levels return toward baseline (Fig. 4*C–E*).

The similarity in the MuSC distribution pattern among neonatal WT mice (Figs. 2*B3* and 6*A5*), *Scnn1b*-Tg mice (Fig. 2*B7*), and OVA-challenged mice (57), namely abundance in the proximal main stem bronchi and a gradual decrease distally, suggests that specific populations of airway epithelial cells are primed to differentiate into MuSC in response to external stimuli. Reports of temporal and spatial expression of transcription factors involved in promoting or suppressing MuSC, such as SPDEF (58) and FOXA2 (59), support this hypothesis.

As quantitated histologically, neonatal IL-4Rα-deficient *Scnn1b*-Tg mice exhibited mucus plugging equivalent to IL-4Rα-sufficient *Scnn1b*-Tg mice, despite decreased MuSC (Fig. 2*C*). Similar results obtained upon prednisolone treatment suggest that airway surface dehydration and defective mucus clearance are major determinants of mucus accumulation over a wide range of MuSC abundance. Moreover, even in WT mice, the high degree of variation in MuSC abundance detected histologically at 5 days, 10 days, and 5 wk of age (Fig. 6, *A* and *B*, and supplemental Fig. 4, *A* and *B*) in comparison to the modest changes observed in BALF total and Muc5b mucins (supplemental Fig. 5, *B* and *C*) suggests that BAL mucin content depends on factors other than the intracellular content of stored mucosubstances alone. We hypothesize that constitutively secreted mucins (40), including Muc5b as detected in BAL (supplemental Fig. 5, *A* and *C*) and shed cell surface mucins (Muc1, Muc4, and Muc16), are an integral part of secreted mucus in WT mice and contribute to mucus obstruction in *Scnn1b*-Tg mouse airways. However, the survival advantage of

IL-4Rα-deficient *Scnn1b*-Tg mice suggests that, especially during the neonatal period, modifications of the mucus secretory system can be beneficial to prevent fatal airway obstruction when mucus clearance is impaired. The absence of significant differences in tracheal epithelial ion transport properties due to the absence of IL-4Rα in *Scnn1b*-Tg mice (supplemental Fig. 2*C*) supports our conclusion that the increased survival of IL-4Rα-deficient *Scnn1b*-Tg mice reflects modifications in MuSC and mucus secretion, not Na^+ transport.

Although IL-4Rα removal had an impact on the neonatal phenotype, lung lesions in adult IL-4Rα-sufficient and -deficient *Scnn1b*-Tg mice were indistinguishable. In contrast to allergen challenge (21) or the late response to viral infection (60), which require the IL-13/IL-4Rα signaling axis to elicit lung pathology, our findings strongly suggest that airway surface dehydration/mucus stasis is a unique stimulus that activates multiple IL-4Rα-independent effector pathways leading to inflammation and remodeling in *Scnn1b*-Tg mice.

Given the complexity of the inflammatory responses in *Scnn1b*-Tg mice, we tested whether a broad-spectrum antiinflammatory agent could ameliorate or reverse adult lung lesions. Glucocorticoids are widely used both clinically and experimentally to blunt inflammation and mucus hypersecretion (27–31, 61, 62), and they can effectively reduce eosinophils, mast cells, $CD4^+$ T lymphocytes, dendritic cells, and proinflammatory cytokines in asthma (63, 64). However, in obstructive lung diseases characterized by neutrophilic inflammation, for example, chronic bronchitis and COPD, inflammation appears to be corticosteroid-resistant (65, 66). In *Scnn1b*-Tg mice, prednisolone treatment blunted eosinophilia and MuSC (Fig. 5*A–C*), similar to other mouse models (62, 67, 68) but did not reduce neutrophil influx, the appearance of large foamy macrophages, or mucus accumulation in the airway lumen. In COPD, unresponsiveness to glucocorticoids has been attributed to inhibition of histone deacetylase 2 activity by oxidative and nitrosative stress (26), a condition that may also occur in *Scnn1b*-Tg mice. Alternatively, glucocorticoids have been shown to spare or enhance innate immunity while repressing adaptive responses (69, 70). We suggest that chronic neutrophil recruitment and macrophage activation are due to a glucocorticoid-insensitive, innate immune response triggered by accumulation of environmental and endogenous stimuli in stagnant mucus, which likely involves signaling through pattern recognition receptors, such as TLRs.

Our studies with neonatal *Scnn1b*-Tg mice and WT littermates led us to discover a temporal and spatial pattern of MuSC and inflammatory cell abundance in the airways of unchallenged WT mice suggestive of an active phase of maturation and adaptation of innate immune responses (Fig. 6). Perinatal changes in MuSC/mucus composition and BAL leukocytes have been described in several species (71–76), including humans (77–81). Surprisingly, we found little information regarding these normal developmental changes in mouse airways. In agreement with our studies, one study that focused on mouse submucosal gland development incidentally showed abundant MuSC in the superficial epithelium at postnatal day 4 (44), and there is one report of eosinophilia in 10-day-old C3HeB/FeJ mice as compared with adult animals (43). Our histological sectioning protocol and the multiple time points studied enabled us to visualize the dynamic changes in MuSC and BAL cells. We hypothesize that immediately after birth, when the acquired immune system is still immature (82, 83), airway mucosal immunity relies on secreted mucus as a primary barrier to protect the host from inhaled, potentially pathogenic particles. A growing body of evidence indicates that neonatal events, for example, bacterial colonization (84, 85), viral infection (86, 87), or allergen exposure (88), have a profound impact on later immune responses. In this context, effective mucus clearance is critical because it determines the concentration and dwell time of particles/pathogens/chemical mediators, the extent of inflammatory and parenchymal cell activation, and the propensity for airway obstruction. While mucus abundance may offer broad airway protection (89), it may become life-threatening when coupled with defective clearance, as in *Scnn1b*-Tg mice. Indeed, different survival rates observed in *Scnn1b*-Tg mice of different genetic backgrounds (Wanda O'Neal, unpublished observation and Ref. 9) likely reflect diversity in the amount/physical properties of secreted mucus or in the architecture of the proximal airways.

In summary, we propose that in neonatal *Scnn1b*-Tg mice, impaired mucus clearance strongly interacts with the normal, IL-4Rα-dependent abundance of MuSC and eosinophils. This interaction produces both potentially lethal mucus obstruction and delays the normal regression of MuSC and eosinophils. In addition to exogenous aerotoxins and endogenous mediators trapped in static mucus, epithelial cell necrosis, transiently present in the lower airways of newborn *Scnn1b*-Tg mice (3), contributes to promote local inflammation (90) and disease onset. Although unresolved/lingering MuSC abundance and eosinophilia can be blunted by corticosteroid treatment, neutrophilia and mucus obstruction persist and are likely responsible for maintaining airway and lung disease in *Scnn1b*-Tg mice. Future studies elucidating the interaction of mucus clearance with other components of airway mucosal immune system during postnatal development, and identifying the molecular mechanisms that sustain airway inflammation and remodeling in adults, will suggest therapeutic approaches for common human obstructive airway diseases.

Acknowledgments

The authors thank Kimberly Burns, Donald Joyner and Tracy Eldred for outstanding technical assistance with histology; Troy Rogers for assistance with Ussing chamber studies; the University of North Carolina Michael Hooker Microscopy Facility, funded by an anonymous private donor, for assistance with imaging; the Thurston Arthritis Research Center, Clinical Proteomics Laboratory (directed by Dr. R. Roubey) for Luminex assays; Dr. Camille Ehre, Dr. Mehmet Kesimer, and Genevieve DeMaria for providing the Muc5b Ab and assistance with the mucin Western blots; Dr. J. Schwabe and Athena Jin for assistance with histology scoring; and Dr. S. L. Tilley for reading the manuscript.

Disclosures

The authors have no financial conflicts of interest.

References

1. Mall, M., B. R. Grubb, J. R. Harkema, W. K. O'Neal, and R. C. Boucher. 2004. Increased airway epithelial Na^+ absorption produces cystic fibrosis-like lung disease in mice. *Nat. Med.* 10: 487–493.
2. Randell, S. H., and R. C. Boucher. 2006. Effective mucus clearance is essential for respiratory health. *Am. J. Respir. Cell Mol. Biol.* 35: 20–28.
3. Mall, M. A., J. R. Harkema, J. B. Trojanek, D. Treis, A. Livraghi, S. Schubert, Z. Zhou, S. M. Kreda, S. L. Tilley, E. J. Hudson, et al. 2008. Development of chronic bronchitis and emphysema in β-epithelial Na^+ channel-overexpressing mice. *Am. J. Respir. Crit. Care Med.* 177: 730–742.
4. Nair, M. G., I. J. Gallagher, M. D. Taylor, P. Loke, P. S. Coulson, R. A. Wilson, R. M. Maizels, and J. E. Allen. 2005. Chitinase and Fizz family members are a generalized feature of nematode infection with selective upregulation of Ym1 and Fizz1 by antigen-presenting cells. *Infect. Immun.* 73: 385–394.
5. Zhu, Z., T. Zheng, R. J. Homer, Y.-K. Kim, N. Y. Chen, L. Cohn, Q. Hamid, and J. A. Elias. 2004. Acidic mammalian chitinase in asthmatic Th2 inflammation and IL-13 pathway activation. *Science* 304: 1678–1682.
6. Homer, R. J., Z. Zhu, L. Cohn, C. G. Lee, W. I. White, S. Chen, and J. A. Elias. 2006. Differential expression of chitinases identify subsets of murine airway epithelial cells in allergic inflammation. *Am. J. Physiol.* 291: L502–L511.
7. Reese, T. A., H. E. Liang, A. M. Tager, A. D. Luster, N. Van Rooijen, D. Voehringer, and R. M. Locksley. 2007. Chitin induces accumulation in tissue of innate immune cells associated with allergy. *Nature* 447: 92–96.
8. Hogg, J. C., F. Chu, S. Utokaparch, R. Woods, W. M. Elliott, L. Buzatu, R. M. Cherniack, R. M. Rogers, F. C. Sciurba, H. O. Coxson, and P. D. Pare.

2004. The nature of small-airway obstruction in chronic obstructive pulmonary disease. *N. Engl. J. Med.* 350: 2645–2653.
9. O'Neal, W. K., A. Livraghi, D. W. Threadgill, E. J. Hudson, M. A. Mall, B. R. Grubb, and R. C. Boucher. 2007. Assessment of genetic modifiers for phenotypic severity of Scnn1b transgenic mice. *Pediatr. Pulmonol.* 30(Suppl.): S266 (Abstr.).
10. Lora, J. M., D. M. Zhang, S. M. Liao, T. Burwell, A. M. King, P. A. Barker, L. Singh, M. Keaveney, J. Morgenstern, J. C. Gutierrez-Ramos, et al. 2005. Tumor necrosis factor-α triggers mucus production in airway epithelium through an IκB kinase β-dependent mechanism. *J. Biol. Chem.* 280: 36510–36517.
11. Busse, P. J., T. F. Zhang, K. Srivastava, B. P. Lin, B. Schofield, S. C. Sealfon, and X. M. Li. 2005. Chronic exposure to TNF-α increases airway mucus gene expression in vivo. *J. Allergy Clin. Immunol.* 116: 1256–1263.
12. Vuillemenot, B. R., J. F. Rodriguez, and G. W. Hoyle. 2004. Lymphoid tissue and emphysema in the lungs of transgenic mice inducibly expressing tumor necrosis factor-α. *Am. J. Respir. Cell Mol. Biol.* 30: 438–448.
13. Fujita, M., J. M. Shannon, C. G. Irvin, K. A. Fagan, C. Cool, A. Augustin, and R. J. Mason. 2001. Overexpression of tumor necrosis factor-α produces an increase in lung volumes and pulmonary hypertension. *Am. J. Physiol.* 280: L39–L49.
14. Churg, A., R. D. Wang, H. Tai, X. Wang, C. Xie, and J. L. Wright. 2004. Tumor necrosis factor-α drives 70% of cigarette smoke-induced emphysema in the mouse. *Am. J. Respir. Crit. Care Med.* 170: 492–498.
15. Nelms, K., A. D. Keegan, J. Zamorano, J. J. Ryan, and W. E. Paul. 1999. The IL-4 receptor: signaling mechanisms and biologic functions. *Annu. Rev. Immunol.* 17: 701–738.
16. Hershey, G. K. 2003. IL-13 receptors and signaling pathways: an evolving web. *J. Allergy Clin. Immunol.* 111: 677–690.
17. Wills-Karp, M. 2004. Interleukin-13 in asthma pathogenesis. *Immunol. Rev.* 202: 175–190.
18. Kelly-Welch, A. E., E. M. Hanson, M. R. Boothby, and A. D. Keegan. 2003. Interleukin-4 and interleukin-13 signaling connections maps. *Science* 300: 1527–1528.
19. Grunig, G., M. Warnock, A. E. Wakil, R. Venkayya, F. Brombacher, D. M. Rennick, D. Sheppard, M. Mohrs, D. D. Donaldson, R. M. Locksley, and D. B. Corry. 1998. Requirement for IL-13 independently of IL-4 in experimental asthma. *Science* 282: 2261–2263.
20. Webb, D. C., A. N. McKenzie, and P. S. Foster. 2001. Expression of the Ym2 lectin-binding protein is dependent on interleukin (IL)-4 and IL-13 signal transduction: identification of a novel allergy-associated protein. *J. Biol. Chem.* 276: 41969–41976.
21. Kuperman, D. A., X. Huang, L. Nguyenvu, C. Holscher, F. Brombacher, and D. J. Erle. 2005. IL-4 receptor signaling in Clara cells is required for allergen-induced mucus production. *J. Immunol.* 175: 3746–3752.
22. Dagenais, A., R. Frechette, Y. Yamagata, T. Yamagata, J. F. Carmel, M. E. Clermont, E. Brochiero, C. Masse, and Y. Berthiaume. 2004. Downregulation of ENaC activity and expression by TNF-α in alveolar epithelial cells. *Am. J. Physiol.* 286: L301–L311.
23. Galietta, L. J., C. Folli, C. Marchetti, L. Romano, D. Carpani, M. Conese, and O. Zegarra-Moran. 2000. Modification of transepithelial ion transport in human cultured bronchial epithelial cells by interferon-γ. *Am. J. Physiol.* 278: L1186–L1194.
24. Coakley, R. D., B. Button, and R. C. Boucher. 2005. Immunoregulation of ion transport and airway surface liquid volume in cultured human CF and NON-CF airway epithelium by TGFβ and TNFα. In *19th North American Cystic Fibrosis Conference. Pediatr. Pulmonol.* 28(Suppl.): 217 (Abstr.).
25. Galietta, L. J. V., P. Pagesy, C. Folli, E. Caci, L. Romio, B. Costes, E. Nicolis, G. Cabrini, M. Goossens, R. Ravazzolo, and O. Zegarra-Moran. 2002. IL-4 is a potent modulator of ion transport in the human bronchial epithelium in vitro. *J. Immunol.* 168: 839–845.
26. Barnes, P. J. 2006. How corticosteroids control inflammation: Quintiles Prize Lecture 2005. *Br. J. Pharmacol.* 148: 245–254.
27. Aoki, M., M. Fukunaga, M. Kitagawa, K. Hayashi, T. Morokata, G. Ishikawa, S. Kubo, and T. Yamada. 2000. Effect of a novel anti-inflammatory compound, YM976, on antigen-induced eosinophil infiltration into the lungs in rats, mice, and ferrets. *J. Pharmacol. Exp. Ther.* 295: 1149–1155.
28. Blyth, D. I., M. S. Pedrick, T. J. Savage, H. Bright, J. E. Beesley, and S. Sanjar. 1998. Induction, duration, and resolution of airway goblet cell hyperplasia in a murine model of atopic asthma: effect of concurrent infection with respiratory syncytial virus and response to dexamethasone. *Am. J. Respir. Cell Mol. Biol.* 19: 38–54.
29. Ikeda, R. K., J. Nayar, J. Y. Cho, M. Miller, M. Rodriguez, E. Raz, and D. H. Broide. 2003. Resolution of airway inflammation following ovalbumin inhalation: comparison of ISS DNA and corticosteroids. *Am. J. Respir. Cell Mol. Biol.* 28: 655–663.
30. El-Hashim, A. Z., D. Wyss, and C. Zuany-Amorim. 2002. Kinetics of airway hyperresponsiveness and airway eosinophilia in BALB/c mice and their modulation by different dexamethasone treatment regimens. *Pulmon. Pharmacol. Ther.* 15: 467–475.
31. Nakao, I., S. Kanaji, S. Ohta, H. Matsushita, K. Arima, N. Yuyama, M. Yamaya, K. Nakayama, H. Kubo, M. Watanabe, et al. 2008. Identification of pendrin as a common mediator for mucus production in bronchial asthma and chronic obstructive pulmonary disease. *J. Immunol.* 180: 6262–6269.
32. Noben-Trauth, N., L. D. Shultz, F. Brombacher, J. F. Urban, Jr., H. Gu, and W. E. Paul. 1997. An interleukin 4 (IL-4)-independent pathway for CD4$^+$ T cell IL-4 production is revealed in IL-4 receptor-deficient mice. *Proc. Natl. Acad. Sci. USA* 94: 10838–10843.
33. Linder, C. C. 2006. Genetic variables that influence phenotype. *ILAR J.* 47: 132–140.
34. Pasparakis, M., L. Alexopoulou, V. Episkopou, and G. Kollias. 1996. Immune and inflammatory responses in TNF alpha-deficient mice: a critical requirement for TNF alpha in the formation of primary B cell follicles, follicular dendritic cell networks and germinal centers, and in the maturation of the humoral immune response. *J. Exp. Med.* 184: 1397–1411.
35. Pfeffer, K., T. Matsuyama, T. M. Kundig, A. Wakeham, K. Kishihara, A. Shahinian, K. Wiegmann, P. S. Ohashi, M. Kronke, and T. W. Mak. 1993. Mice deficient for the 55 kd tumor necrosis factor receptor are resistant to endotoxic shock, yet succumb to *L. monocytogenes* infection. *Cell* 73: 457–467.
36. Shore, S. A., J. H. Abraham, I. N. Schwartzman, G. G. K. Murthy, and J. D. Laporte. 2000. Ventilatory responses to ozone are reduced in immature rats. *J. Appl. Physiol.* 88: 2023–2030.
37. Kirkham, S., J. K. Sheehan, D. Knight, P. S. Richardson, and D. J. Thornton. 2002. Heterogeneity of airways mucus: variations in the amounts and glycoforms of the major oligomeric mucins MUC5AC and MUC5B. *Biochem. J.* 361: 537–546.
38. Thornton, D. J., I. Carlstedt, M. Howard, P. L. Devine, M. R. Price, and J. K. Sheehan. 1996. Respiratory mucins: identification of core proteins and glycoforms. *Biochem. J.* 316(Pt 3): 967–975.
39. Sheehan, J. K., R. P. Boot-Handford, E. Chantler, I. Carlstedt, and D. J. Thornton. 1991. Evidence for shared epitopes within the "naked" protein domains of human mucus glycoproteins: a study performed by using polyclonal antibodies and electron microscopy. *Biochem. J.* 274(Pt. 1): 293–296.
40. Zhu, Y., C. Ehre, L. H. Abdullah, J. K. Sheehan, M. Roy, C. M. Evans, B. F. Dickey, and C. W. Davis. 2008. Munc13-2$^{-/-}$ baseline secretion defect reveals source of oligomeric mucins in mouse airways. *J. Physiol.* 586: 1977–1992.
41. Nguyen, L. P., O. Omoluabi, S. Parra, J. M. Frieske, C. Clement, Z. Ammar-Aouchiche, S. B. Ho, C. Ehre, M. Kesimer, B. J. Knoll, et al. 2008. Chronic exposure to beta-blockers attenuates inflammation and mucin content in a murine asthma model. *Am. J. Respir. Cell Mol. Biol.* 38: 256–262.
42. Grubb, B. R. 2002. Bioelectric measurement of CFTR function in mice. *Methods Mol. Med.* 70: 525–535.
43. George, C. L., M. L. White, K. Kulhankova, A. Mahajan, P. S. Thorne, J. M. Snyder, and J. N. Kline. 2006. Early exposure to a nonhygienic environment alters pulmonary immunity and allergic responses. *Am. J. Physiol.* 291: L512–L522.
44. Rawlins, E. L., and B. L. Hogan. 2005. Intercellular growth factor signaling and the development of mouse tracheal submucosal glands. *Dev. Dyn.* 233: 1378–1385.
45. Liu, X., R. R. Driskell, and J. F. Engelhardt. 2004. Airway glandular development and stem cells. *Curr. Top. Dev. Biol.* 64: 33–56.
46. Webb, D. C., Y. Cai, K. I. Matthaei, and P. S. Foster. 2007. Comparative roles of IL-4, IL-13, and IL-4Rα in dendritic cell maturation and CD4$^+$ Th2 cell function. *J. Immunol.* 178: 219–227.
47. Webb, D. C., K. I. Matthaei, Y. Cai, A. N. McKenzie, and P. S. Foster. 2004. Polymorphisms in IL-4Rα correlate with airways hyperreactivity, eosinophilia, and Ym protein expression in allergic IL-13$^{-/-}$ mice. *J. Immunol.* 172: 1092–1098.
48. Miner, J. N. 2002. Designer glucocorticoids. *Biochem. Pharmacol.* 64: 355–361.
49. Rowe, S. M., P. L. Jackson, G. Liu, M. Hardison, A. Livraghi, G. M. Solomon, D. B. McQuaid, B. D. Noerager, A. Gaggar, J. P. Clancy, et al. 2008. Potential role of high-mobility group box 1 in cystic fibrosis airway disease. *Am. J. Respir. Crit. Care Med.* 178: 822–831.
50. Jiang, D., J. Liang, and P. W. Noble. 2007. Hyaluronan in tissue injury and repair. *Annu. Rev. Cell. Dev. Biol.* 23: 435–461.
51. Temelkovski, J., S. P. Hogan, D. P. Shepherd, P. S. Foster, and R. K. Kumar. 1998. An improved murine model of asthma: selective airway inflammation, epithelial lesions and increased methacholine responsiveness following chronic exposure to aerosolised allergen. *Thorax* 53: 849–856.
52. Zosky, G. R., and P. D. Sly. 2007. Animal models of asthma. *Clin. Exp. Allergy* 37: 973–988.
53. Moghaddam, S. J., C. G. Clement, M. M. De la Garza, X. Zou, E. L. Travis, H. W. Young, C. M. Evans, M. J. Tuvim, and B. F. Dickey. 2008. *Haemophilus influenzae* lysate induces aspects of the chronic obstructive pulmonary disease phenotype. *Am. J. Respir. Cell Mol. Biol.* 38: 629–638.
54. Harrod, K. S., and R. J. Jaramillo. 2002. *Pseudomonas aeruginosa* and tumor necrosis factor-α attenuate Clara cell secretory protein promoter function. *Am. J. Respir. Cell Mol. Biol.* 26: 216–223.
55. Lee, J. J., D. Dimina, M. P. Macias, S. I. Ochkur, M. P. McGarry, K. R. O'Neill, C. Protheroe, R. Pero, T. Nguyen, S. A. Cormier, et al. 2004. Defining a link with asthma in mice congenitally deficient in eosinophils. *Science* 305: 1773–1776.
56. Humbles, A. A., C. M. Lloyd, S. J. McMillan, D. S. Friend, G. Xanthou, E. E. McKenna, S. Ghiran, N. P. Gerard, C. Yu, S. H. Orkin, and C. Gerard. 2004. A critical role for eosinophils in allergic airways remodeling. *Science* 305: 1776–1779.
57. Evans, C. M., O. W. Williams, M. J. Tuvim, R. Nigam, G. P. Mixides, M. R. Blackburn, F. J. DeMayo, A. R. Burns, C. Smith, S. D. Reynolds, et al. 2004. Mucin is produced by Clara cells in the proximal airways of antigen-challenged mice. *Am. J. Respir. Cell Mol. Biol.* 31: 382–394.
58. Park, K.-S., T. R. Korfhagen, M. D. Bruno, J. A. Kitzmiller, H. Wan, S. E. Wert, G. K. Khurana Hershey, G. Chen, and J. A. Whitsett. 2007. SPDEF regulates goblet cell hyperplasia in the airway epithelium. *J. Clin. Invest.* 117: 978–988.
59. Wan, H., K. H. Kaestner, S. L. Ang, M. Ikegami, F. D. Finkelman, M. T. Stahlman, P. C. Fulkerson, M. E. Rothenberg, and J. A. Whitsett. 2004.

Foxa2 regulates alveolarization and goblet cell hyperplasia. *Development*131: 953–964.
60. Kim, E. Y., J. T. Battaile, A. C. Patel, Y. You, E. Agapov, M. H. Grayson, L. A. Benoit, D. E. Byers, Y. Alevy, J. Tucker, et al. 2008. Persistent activation of an innate immune response translates respiratory viral infection into chronic lung disease. *Nat. Med.* 14: 633–640.
61. Barnes, P. J. 2006. Corticosteroids: the drugs to beat. *Eur. J. Pharmacol.* 533: 2–14.
62. Rogers, D. F., and P. J. Barnes. 2006. Treatment of airway mucus hypersecretion. *Ann. Med.* 38: 116–125.
63. Belvisi, M. G. 2004. Regulation of inflammatory cell function by corticosteroids. *Proc. Am. Thorac. Soc.* 1: 207–214.
64. Chanez, P., A. Bourdin, I. Vachier, P. Godard, J. Bousquet, and A. M. Vignola. 2004. Effects of inhaled corticosteroids on pathology in asthma and chronic obstructive pulmonary disease. *Proc. Am. Thorac. Soc.* 1: 184–190.
65. Donohue, J. F., and J. A. Ohar. 2004. Effects of corticosteroids on lung function in asthma and chronic obstructive pulmonary disease. *Proc. Am. Thorac. Soc.* 1: 152–160.
66. Hargreave, F. E. 2007. Quantitative sputum cell counts as a marker of airway inflammation in clinical practice. *Curr. Opin. Allergy Clin. Immunol.* 7: 102–106.
67. Rogers, D. F., and P. K. Jeffery. 1986. Inhibition of cigarette smoke-induced airway secretory cell hyperplasia by indomethacin, dexamethasone, prednisolone, or hydrocortisone in the rat. *Exp. Lung Res.* 10: 285–298.
68. Rogers, D. F. 1994. Airway goblet cells: responsive and adaptable front-line defenders. *Eur. Respir. J.* 7: 1690–1706.
69. Stellato, C. 2007. Glucocorticoid actions on airway epithelial responses in immunity: functional outcomes and molecular targets. *J. Allergy Clin. Immunol.* 120: 1247–1263.
70. Schleimer, R. P. 2004. Glucocorticoids suppress inflammation but spare innate immune responses in airway epithelium. *Proc. Am. Thorac. Soc.* 1: 222–230.
71. Randell, S. H., T. Shimizu, W. Bakewell, F. C. Ramaekers, and P. Nettesheim. 1993. Phenotypic marker expression during fetal and neonatal differentiation of rat tracheal epithelial cells. *Am. J. Respir. Cell Mol. Biol.* 8: 546–555.
72. Otani, E. M., C. Newkirk, and E. M. McDowell. 1986. Development of hamster tracheal epithelium: IV. Cell proliferation and cytodifferentiation in the neonate. *Anat. Rec.* 214: 183–192.
73. Leigh, M. W., T. M. Gambling, J. L. Carson, A. M. Collier, R. E. Wood, and T. F. Boat. 1986. Postnatal development of tracheal surface epithelium and submucosal glands in the ferret. *Exp. Lung Res.* 10: 153–169.
74. Winkle, L. S. V., M. V. Fanucchi, L. A. Miller, G. L. Baker, L. J. Gershwin, E. S. Schelegle, D. M. Hyde, M. J. Evans, and C. G. Plopper. 2004. Epithelial cell distribution and abundance in rhesus monkey airways during postnatal lung growth and development. *J. Appl. Physiol.* 97: 2355–2363.
75. Yu, M., X. Zheng, J. Peake, J. P. Joad, and K. E. Pinkerton. 2008. Perinatal environmental tobacco smoke exposure alters the immune response and airway innervation in infant primates. *J. Allergy Clin. Immunol.* 122: 640–647.
76. Plopper, C. G., G. E. Hatch, V. Wong, X. Duan, A. J. Weir, B. K. Tarkington, R. B. Devlin, S. Becker, and A. R. Buckpitt. 1998. Relationship of inhaled ozone concentration to acute tracheobronchial epithelial injury, site-specific ozone dose, and glutathione depletion in rhesus monkeys. *Am. J. Respir. Cell Mol. Biol.* 19: 387–399.
77. Matsuba, K., and W. M. Thurlbeck. 1972. A morphometric study of bronchial and bronchiolar walls in children. *Am. Rev. Respir. Dis.* 105: 908–913.
78. Jeffery, P. K., D. Gaillard, and S. Moret. 1992. Human airway secretory cells during development and in mature airway epithelium. *Eur. Respir. J.* 5: 93–104.
79. Lamb, D., and L. Reid. 1972. Acidic glycoproteins produced by the mucous cells of the bronchial submucosal glands in the fetus and child: a histochemical autoradiographic study. *Br. J. Dis. Chest* 66: 248–253.
80. Grigg, J., J. Riedler, C. F. Robertson, W. Boyle, and S. Uren. 1999. Alveolar macrophage immaturity in infants and young children. *Eur. Respir. J.* 14: 1198–1205.
81. Ratjen, F., M. Bredendiek, M. Brendel, J. Meltzer, and U. Costabel. 1994. Differential cytology of bronchoalveolar lavage fluid in normal children. *Eur. Respir. J.* 7: 1865–1870.
82. Holt, P. G., J. W. Upham, and P. D. Sly. 2005. Contemporaneous maturation of immunologic and respiratory functions during early childhood: implications for development of asthma prevention strategies. *J. Allergy Clin. Immunol.* 116: 16–24.
83. Adkins, B., C. Leclerc, and S. Marshall-Clarke. 2004. Neonatal adaptive immunity comes of age. *Nat. Rev. Immunol.* 4: 553–564.
84. Bisgaard, H., M. N. Hermansen, F. Buchvald, L. Loland, L. B. Halkjaer, K. Bonnelykke, M. Brasholt, A. Heltberg, N. H. Vissing, S. V. Thorsen, et al. 2007. Childhood asthma after bacterial colonization of the airway in neonates. *N. Engl. J. Med.* 357: 1487–1495.
85. von Mutius, E. 2007. Of attraction and rejection: asthma and the microbial world. *N. Engl. J. Med.* 357: 1545–1547.
86. Culley, F. J., J. Pollott, and P. J. Openshaw. 2002. Age at first viral infection determines the pattern of T cell-mediated disease during reinfection in adulthood. *J. Exp. Med.* 196: 1381–1386.
87. Holt, P. G., and P. D. Sly. 2002. Interactions between RSV infection, asthma, and atopy: unraveling the complexities. *J. Exp. Med.* 196: 1271–1275.
88. Illi, S., E. von Mutius, S. Lau, B. Niggemann, C. Gruber, and U. Wahn. 2006. Perennial allergen sensitisation early in life and chronic asthma in children: a birth cohort study. *Lancet* 368: 763–770.
89. Linden, S. K., P. Sutton, N. G. Karlsson, V. Korolik, and M. A. McGuckin. 2008. Mucins in the mucosal barrier to infection. *Mucosal Immunol.* 1: 183–197.
90. Chen, C. J., H. Kono, D. Golenbock, G. Reed, S. Akira, and K. L. Rock. 2007. Identification of a key pathway required for the sterile inflammatory response triggered by dying cells. *Nat. Med.* 13: 851–856.